

Influence of thermal treatment on the structure of an isotactic polypropylene

Lysiane Poussin^{a,*}, Yves A. Bertin^a, Jacques Parisot^a and Claude Brassy^b

^aLaboratoire de Mécanique et de Physique des Matériaux, URA CNRS 863, ENSMA, BP 109, 86960 Futuroscope Cedex, France

^bLaboratoire de Combustion et de Détonique, UPR CNRS 9028, ENSMA, BP 109, 86960 Futuroscope Cedex, France

(Received 14 April 1994; revised 16 January 1996)

The structural evolution of an industrial polypropylene polymer is studied as a function of the duration of annealing at 398 K by four methods: wide angle X-ray diffraction (WAXS), infrared absorption spectroscopy, density measurements and differential scanning calorimetry (d.s.c.). We observe a very quick variation of several structural parameters such as crystallinity, density and apparent crystal size, exhibiting a real improvement of the structure, as early as the first five minutes of treatment. A refinement of the crystal unit cell parameters during the annealing completes the data. Finally, conclusions derived according to the different methods are compared. © 1998 Elsevier Science Ltd. All rights reserved.

(Keywords: polypropylene; annealing; WAXS)

INTRODUCTION

Fatigue behaviour of semi-crystalline polymers is largely improved by an increase in the crystallization rate¹. For an isotactic polypropylene (iPP), an annealing of 2 h at 398 K, leading to a 10% increase in the crystallinity, induces, at low stress levels, an increase of a factor of 3–10 in the fatigue life. At higher stresses, the fatigue lifetime remains unchanged². Such a heat treatment might cause structural and morphological modifications of the material on different scales, such as:

- macromolecular chain;
- lamellae arrangement, separated by amorphous phase (crystal growth, lamellae structure modification);
- long distance organization of crystalline lamellae and amorphous interlamellae zones;
- bulk sample, which can show either a homogeneous microstructure (spherulitic, for example) or a heterogeneous microstructure (core-skin morphology for injected pieces).

The temperature was chosen according to the work of Monasse³. In his study, three stages of crystal growth were observed in the morphological and thermodynamic evolution of the iPP specimen, related to the crystallization temperature. His interpretation was that, at the upper crystallization temperature (stage I), chain folding was organized at the lamellae surface, whereas at lower temperatures (stages II and III), chains were less organized at the surface of lamellae, yielding to links between amorphous and crystalline phases. The temperature chosen in the present study corresponds to stage II as defined above.

The aim of this work is to characterize the change of microcrystalline structure of an industrial isotactic poly-

propylene during successive annealings at 398 K, by means of different physical analytical methods: wide angle X-ray diffraction (WAXS), infrared absorption, densitometry, and differential scanning calorimetry (d.s.c.).

EXPERIMENTAL

Sample preparation

The material studied was an industrial isotactic polypropylene manufactured by ATOCHEM (3050 MN1) with a molecular mass, M_n , of 55 000. Pellets of the polymer were subsequently processed by intrusion⁴ in a thick mould ($300 \times 200 \times 5 \text{ mm}^3$) designed for producing parallelepipedic plates. The melt, heated to 503 K, was extruded into the mould, which was kept at 302 K. Mould feeding was continued during the cooling sequence, under a pressure kept constant at 6 MPa. The cooling time was about 240 s. The plates obtained thereby had a negligible orientation and much less chain degradation or bubbles than from conventional injection or extrusion techniques. Besides, the cooling rate was relatively slow and the semi-crystalline structure was quite reproducible. Rectangular parallelepipedic samples ($40 \times 10 \times 5 \text{ mm}^3$) were cut from these plates. Although the orientation induced by that process was minimal, we took care that the length of the samples was always parallel to the direction of intrusion.

Heat treatment

The thermal treatment consisted of successive annealing at 398 K in air, for a total time ranging between 5 minutes and 31 days. As shown in *Table 1*, W samples were subjected to several short annealing times, whereas U samples were subjected to several longer annealing times. The temperature was measured by a thermocouple placed in a small hole inside the central part of the sample; this showed that the specimens rapidly (in less than 20 s)

* To whom correspondence should be addressed

Table 1 Thermal treatment times at 398 K for W and U samples: the W sample was treated with short successive annealing times, the U sample with longer successive annealing times

| Sample name | Successive annealing time (min) | Total annealing time (min) |
|-------------|---------------------------------|----------------------------|
| W | 0 | 0 |
| W5m | 5 | 5 |
| W10m | 5 | 10 |
| W15m | 5 | 15 |
| W20m | 5 | 20 |
| W30m | 10 | 30 |
| W45m | 15 | 45 |
| W1h45 | 60 | 105 |
| W3h | 75 | 180 |
| W6h | 180 | 360 |
| W12h | 360 | 720 |
| Sample name | Successive annealing time (h) | Total annealing time (h) |
| U | 0 | 0 |
| U30m | 0.5 | 0.5 |
| U1h | 0.5 | 1 |
| U2h | 1 | 2 |
| U5h | 3 | 5 |
| U11h | 6 | 11 |
| U24h | 13 | 24 |
| U48h | 24 | 48 |
| U75h | 27 | 75 |
| U171h | 96 | 171 |
| U31d | 573 | 744 |

reached the oven temperature which was kept at 398 K. At the end of each annealing step, the samples were quenched in air at room temperature in order to freeze the structural organization reached. The samples were then stored at room temperature before further analysis. This rapid change of temperature allowed us to assume an isothermal evolution of the material only during heat treatment and not at room temperature.

WAXS

Wide angle X-ray diffraction spectra were recorded on a Siemens Kristalloflex 710 diffractometer equipped with a chromium anode tube ($\lambda_{\text{CrK}\alpha 1} = 2.28975 \text{ \AA}$) and a scintillation counter. The recording conditions were:

- counting step: $s = 0.02^\circ$
- counting time per step: $t = 3 \text{ s}$
- scanning angular sector 2θ : 15° – 45°
- split width: 1°
- recording time: 1 h 20 min
- diffracting material thickness: 0.8 mm

Data analysis was carried out using Siemens Diffract software package containing EVA and FIT (interactive profile fitting) programmes. The refinement of the crystalline unit cell parameters by the least-squares method was done with AFDPA⁵ software.

Density measurements

The density (ρ) was measured using Archimedes' principle. A Sartorius balance of precision 10^{-5} g was used:

$$\rho = \frac{W(a) \cdot [\rho(f) + 0.00120]}{0.99983 \cdot [W(a) - W(f)]}$$

where $W(a)$ and $W(f)$ represented respectively the sample mass in air and in water, $\rho(f)$ the water density allowing for the actual temperature of the water, measured to $\pm 0.1 \text{ K}$

with a mercury thermometer, between 293 and 296 K. 0.00120 and 0.99983 were two coefficients linked to the balance.

Differential scanning calorimetry (d.s.c.)

Differential scanning calorimetry measurements were carried out over the temperature range 283–463 K using a Mettler TA 30 d.s.c. purged with nitrogen and cooled with liquid nitrogen. Runs were carried out on samples of about 10 mg at a heating rate of 10 K min^{-1} . Endotherms were recorded during the heating cycle.

Infrared spectroscopy

A Nicolet 510 FTi.r. spectrophotometer was used to record infrared spectra between 700 and 1550 cm^{-1} . The sample thickness was cut to $20 \mu\text{m}$ with a microtome. The spectra were measured over 10 scans.

RESULTS

Wide angle X-ray diffraction (WAXS) measurements on untreated samples and all annealed samples exhibited only the monoclinic α form^{6,7} of iPP. The evolution of polymer structure with annealing at 398 K was characterized by the evolution of diffractograms.

Figure 1 shows several diffractograms, representing the diffracted intensities versus the diffraction angle 2θ , for an untreated sample (W), for one annealed for 5 min (W5m), and for one totally annealed for 12 h (W12h). Figure 2

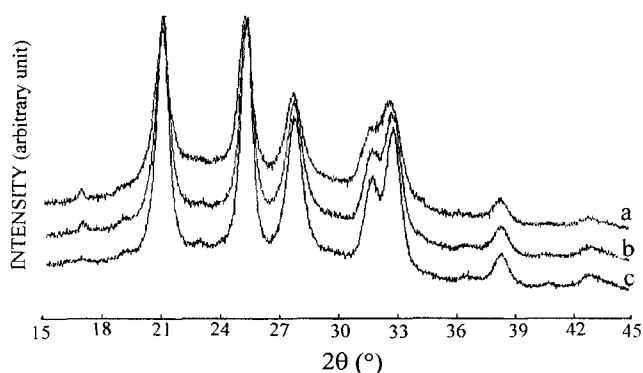


Figure 1 WAXS diffractograms for short annealing times at 398 K corresponding to: (a) untreated sample (W); (b) 5 min annealed (W5m); (c) 12 h annealed (W12h). The most important part of the evolution takes place during the first five minutes of annealing at 398 K

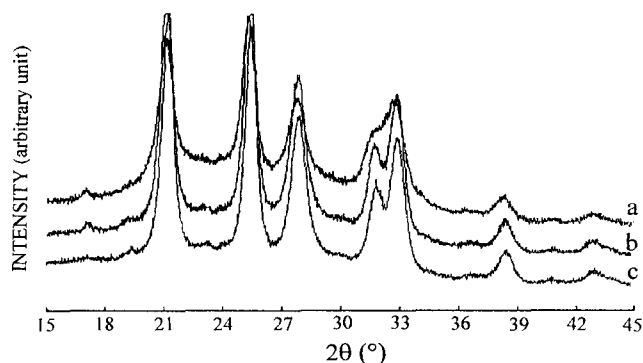


Figure 2 WAXS diffractograms for long annealing times at 398 K corresponding to: (a) untreated sample (U); (b) 5 h annealed (U5h); (c) 75 h annealed (U75h). X-ray spectra do not seem to change significantly, showing a stabilization of the polymer structure

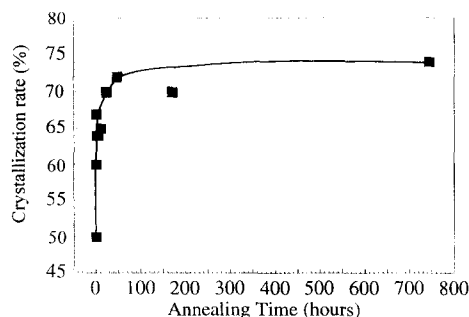


Figure 3 WAXS crystallinity versus annealing time at 398 K

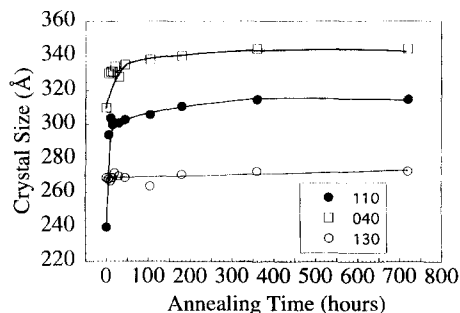


Figure 4 Crystal sizes perpendicular to (110), (040) and (130) planes versus annealing time at 398 K

shows the diffractograms for the untreated sample (U), for a sample totally annealed for 5 h (U5h), and for one totally annealed for 75 h (U75h).

The most important features of the structural changes occurring during the first five minutes of annealing at 398 K are:

- a slight increase in the relative intensities of the (hkl) reflections;
- an inversion in the relative intensities of 110 and 040 peaks;
- a significant decrease in the amorphous contribution;
- a better separation between the 111 reflections of the $13\bar{1}$ and 041 doublet;
- a slight shift of (hkl) reflections to higher 2θ values.

For longer annealing times, the X-ray spectra do not seem to change significantly, showing a stabilization of the polymer structure.

The crystallization rate, X , was measured by the Weidinger and Hermans method⁸ where the area of the crystalline peaks, obtained after subtracting the amorphous area, is compared with the total area of the pattern. Figure 3 shows the rapid variation of crystallinity versus the total duration of annealing. This is in accordance with the literature, where a rapid increase in the crystallization rate was observed over an annealing temperature of 393 K⁹, resulting in increased perfection of the monoclinic phase.

The organized domain dimension was deduced from the Scherrer equation¹⁰: $L = \lambda / (D \cos \theta)$, where L represents the apparent crystal size in Å, λ the wavelength used, D the half-height angular width, and θ the position of the family of diffracting (hkl) planes. As shown in Figure 4, the size does not change in the [130] direction, whatever the annealing time. On the other hand, in the [110] and [040] crystallographic directions, an important and rapid increase in crystal size, followed by a plateau, is observed, confirming Vittoria's results⁹ obtained on 0.2 mm films.

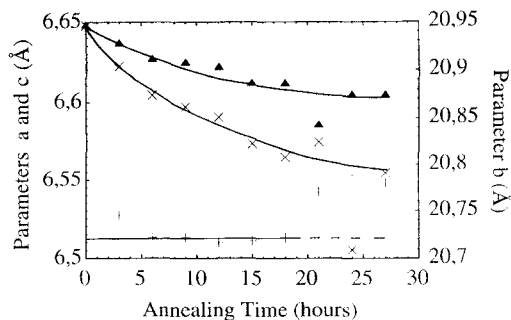


Figure 5 Unit cell parameters versus annealing time at 398 K: (▲) parameter a; (×) parameter b; (+) parameter c

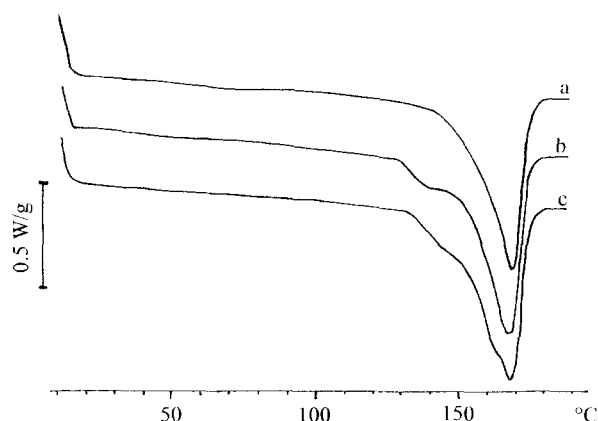


Figure 6 D.s.c. endotherms: (a) untreated sample; (b) 2 h annealed; (c) 24 h annealed (scales of the y-axis change from one curve to another)

The variation of crystal parameters a , b , c , can be seen according to a pattern fitting on the (111), $(13\bar{1})$ and (041) planes, corresponding to neighbouring diffraction angles. The FIT programme performed a profile fitting using the least-squares method. A function of the following type was used: $f(x) = P_1(x) + P_2(x) + \dots + P_n(x) + B(x)$, where n is the number of peaks, and B is the continuous background which was assumed to be, locally, a straight line. Pearson's VII function, using the Cauchy function for the peaks P_i , was chosen for its better reliability coefficient. The refinement of crystal unit cell parameters a , b , c and angle β was obtained with AFPAR software⁵, from experimental angular positions 2θ found by FIT and from Natta's parameters⁶ ($a = 6.65$, $b = 20.95$ and $c = 6.50$ Å; $\beta = 99.30^\circ$).

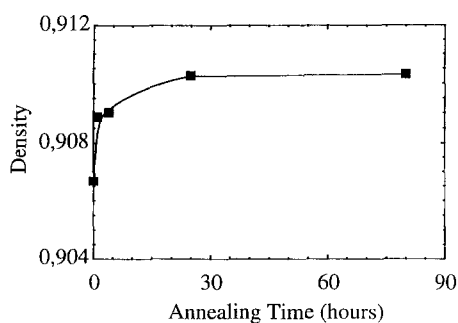
Figure 5 shows (a, b, c) variations versus annealing time at 398 K. During the first 18 h of treatment, a relative decrease of the a and b parameters by 0.6% and 0.7% respectively is observed. During the same time, the c parameter remains constant. Beyond 18 h at 398 K, a fluctuation of b and an apparent increase of c are noticed.

Other analytical methods exhibited the same trends as WAXS measurements.

D.s.c. heating curves for the iPP samples, respectively untreated, annealed 2 h and 24 h, are shown in Figure 6. The main melting temperature was always close to 443 K. The shape of the endotherm of the untreated sample seems to be simple, but, after annealing, small shoulders appear on the lower temperature part, indicating a microstructural evolution generated by the heat treatment. The experimental melting enthalpy³, $\Delta H = 148$ kJ mol⁻¹, yielded to the d.s.c. crystallinity given in Table 2. Density was found to increase during annealing (Figure 7), which is interpreted to mean an

Table 2 WAXS, density, DCS, and IR crystallinities for several annealing times at 398 K: for the untreated sample, the DSC and density crystallinities are higher than WAXS crystallinity, revealing a possible phase system, as explained in the discussion

| | Untreated sample | Annealing 2 h | Annealing 3 h | Annealing 24 h |
|--------------------------------------------------------------|------------------|------------------|------------------|----------------|
| WAXS ⁸ | 46% | 62% | 63% | 69% |
| Density ¹³ | 63% | – | 68% | 68% |
| $X\% = 100 \times \frac{(\rho - \rho_a)}{(\rho_c - \rho_a)}$ | | | | |
| DSC ³ | 56% | 63% | – | 66% |
| $X\% = 100 \times \frac{\Delta H_f}{148}$ | | | | |
| IR ¹⁶ | 52% | – | 71% | – |
| $X\% = \frac{990(D_{846}/D_{1171}) + 80}{13.6}$ | | | | |


Figure 7 Density versus annealing time at 398 K

increase in the crystallinity since the crystalline phase is more dense than the amorphous part. The crystallization rate was calculated from these data, using the amorphous density ρ_a and crystal density ρ_c given by Natale *et al.*¹¹ ($\rho_a = 0.856 \text{ g cm}^{-3}$, $\rho_c = 0.936 \text{ g cm}^{-3}$): it increases with annealing time, as seen in Table 2. One can expect an increase of density due to physical ageing of material at ambient temperature; such phenomena have been observed by Struik¹² using creep tests, and by Kovacs and Hutchinson¹³ using volume measurements on amorphous materials.

Infrared crystallinity, reported in Table 2 was calculated by Bourriot's method¹⁴ which considers the ratio of optical density of a crystalline band D_{846} and a reference band D_{1171} taken as internal standard.

DISCUSSION

A semi-crystalline polymer is locally a periodic arrangement of chains in crystalline lamellae, linked together by amorphous zones. Isotactic polypropylene exhibits a spherulitic texture, built up of radial and tangential crystallites, as shown by Monasse³, merged into the amorphous phase. Three distinct models of macromolecular chain organization on crystalline lamellae surfaces have been proposed. The mixed organization with adjacent and non-adjacent folds and stretched chains seems the more likely³.

A temperature of 398 K favours molecular mobility in the amorphous phases, and the motion of the chains leads to a more stable thermodynamic position. Better organization of amorphous chains leads to the formation of zones in which the molecular arrangement is close to the crystal organization. In these zones, thermoactive germs from which crystals can grow could exist. D.s.c. shoulders on Figure 7 are probably due to the fusion of such microcrystalline zones^{15,16}. According to Monasse³, these microcrystalline zones may be organized in tangential lamellae. At the same time, the growth of radial crystallites begins by adding new unit cells from the amorphous domains close to the organized one. The shift to higher temperatures and the broadening of the first d.s.c. shoulder, for annealing times of 2 h and 24 h, seems to indicate an increase in size of incipient crystalline lamellae towards the average size of pre-existing ones. The growth of new crystallites is faster than that of those already present. This rapid increase in size of the organized domains with annealing is confirmed by the increase of the crystallization rate (Table 2) and the crystal size (Figure 4).

In Table 2, the crystallinity obtained by d.s.c., density and i.r. methods is compared with the X-ray measured crystallinity. The comparison shows that, for the untreated sample, WAXS crystallinity is clearly lower than that measured by any other method. The differences are too high, particularly with the density and d.s.c. results, to be disregarded. On the other hand, for the specimen annealed for 24 h, these differences become negligible. The discrepancy of the crystallinity of the untreated sample measured by the different methods can be explained as follows. During the cooling process in the mould, small zones with a smectic organization^{9-11,15,16} can be formed in the amorphous part, giving a three-phase system. In the diffracting material volume, these imperfectly organized microdomains have a negligible diffracted intensity in comparison with the diffracted intensity of the main crystallites. Besides, this diffracted intensity should concern only some diffraction peaks. For this reason, the X-ray crystallinity seems weak. On one hand, using the d.s.c. method, as the untreated material is not quite stable at temperatures close to the main melting peak, the diagram may be slightly distorted by some parasitic local phenomena of crystallization and melting. On the other hand, all crystallites, even the

smallest ones in the smectic phase, contribute to the total thermal result, leading to a higher crystallinity; thus the crystallinity derived from densitometric measurements as reported in Table 2 is not right. The density d should really be given by:

$$\frac{1}{d} = \frac{\alpha_a}{d_a} + \frac{\alpha_{sm}}{d_{sm}} + \frac{\alpha_c}{d_c}$$

where α_a , α_{sm} , α_c are respectively the mass fractions of the amorphous, smectic and crystalline components which can be obtained from absorption measurements¹¹. For the sample annealed for 3 h at 398 K, the crystallinity from density measurement is still higher than that from X-ray measurement. This may result from the smectic phase not being completely transformed into the monoclinic phase. After 24 h at 398 K, the crystallinity results obtained by the different methods are in good agreement, revealing better organization of all the smectic phase.

Another consequence of thermal agitation would be a slight shift of atomic positions in the unit cell, inducing a fluctuation of structural factors of planes, without any change of spatial group. As the diffracted intensity is proportional to the square of the structural factor, these fluctuations explain the inversion of the relative intensities of the (110) and (040) peaks observed in Figures 1 and 2. It would be interesting to calculate the atomic positions and to refine them, but we are limited by the insufficient number of reflections.

Furthermore, the annealing temperature could explain the contraction of the a and b unit cell parameters by better contact of atoms, contributing to increased density. Previously, after several annealings at 443 K, Smadja¹⁷ observed a shift of peaks to slightly higher values of 2θ , related to a decrease of the b parameter only, i.e. involving a retraction of the unit cell in one dimension. Recently, from a melted and recrystallized polypropylene sample, Cheng¹⁸ showed a decrease of both a and b parameters with crystallization temperature. The c parameter remained unchanged.

CONCLUSION

The annealing of isotactic polypropylene leads to structural modifications associated with a better organization of the

material. Different analytical methods (WAXS, densitometry, d.s.c. and i.r.) showed an increase in crystallinity and crystal size, as well as a variation of a and b unit cell parameters, as early as the first 5 min at 398 K. Rapid evolution to a more stable thermodynamic state is very likely the main source of improvement in fatigue life. For this reason, such investigations should be used during fatigue tests to establish a link between polymer crystalline structure and dissipation phenomena.

ACKNOWLEDGEMENTS

The authors thank ATOCHEM (CERTADO, Serquigny, France) for kindly providing the polypropylene plates, Mr Jeanne of CRITT Matériaux (Rochefort Sur Mer) for d.s.c. measurements, and Mrs PETIT of Laboratoire de Pétrologie (Université de Poitiers) for i.r. measurements.

REFERENCES

1. Hertzberg, R. W. and Manson, J. A., *Fatigue of Engineering Plastics*. Academic Press, New York, 1980.
2. Cailleau, P., Thesis, Poitiers, France, 1996.
3. Monasse, B., Thesis No. 8701, Lyon, France, 1987.
4. Aboulfaraj, M., Ulrich, B., Dahoun, A. and G'Sell, C., *Polymer*, 1993, **34**, 4817.
5. Lestienne, B., Saux, M. and VDM, R., AFPAR software, 1990.
6. Natta, G. and Corradini, P., *Nuovo Cim., Suppl.*, 1960, **15**, 40.
7. Mencik, Z., *J. Macromol. Sci.—Phys.*, 1972, **B6**, 101.
8. Weidinger, A. and Hermans, P. H., *Macromol. Chem.*, 1961, **50**, 98.
9. Vittoria, V., *J. Macromol. Sci.—Phys.*, 1989, **B28**(3&4), 489.
10. Guinier, A., Bouriot, P., Hagege, R. and Sotton, M., *Bull. Sci. ITF*, 1976, **5**, 139.
11. Natale, R., Russo, R. and Vittoria, V., *J. Mat. Sci.*, 1992, **27**, 4350.
12. Struik, L. C. E., *Physical Aging in Amorphous Polymers and Other Materials*, pp. 52–56. Elsevier, Amsterdam, 1978.
13. Kovacs, A. J. and Hutchinson, J. M., in *The Structure of Non-crystalline Materials*, ed. P. H. Gaskell. Taylor & Francis, London, 1977.
14. Bouriot, P., Hagege, R. and Sotton, M., *Bull. Sci. ITF*, 1976, **5**, 139.
15. Jourdan, C., Cavaille, J. Y. and Perez, J., *J. Polym. Sci., Part B: Polym. Phys.*, 1989, **27**, 2361.
16. Oulad Bouyahya Idrissi, M., Thesis No 1391, Lyon I, France, 1983.
17. Smadja, C., Thesis No. 260, Lyon, France, 1967.
18. Cheng, S. Z. D., Janimak, J. J., Zhang, A. and Hsieh, E. T., *Polymer*, 1991, **32**, 648.